Hierarchical Macroporosity Induced by Constrained Syneresis in Core−Shell Polysaccharide Composites

Francesco Di Renzo,* Romain Valentin, Michel Boissière,† Audrey Tourrette, Giuseppe Sparapano, Karine Molvinger, Jean-Marie Devoisselle, Corine Gérardin, and Françoise Quignard

Laboratoire de Matériaux Catalytiques et Catalyse en Chimie Organique, UMR 5618 CNRS-ENSCM-UM1, Institut C. Gerhardt, FR 1878, ENSCM, 8 rue Ecole Normale, 34296 Montpellier, France

Received February 16, 2005. Revised Manuscript Received June 18, 2005

A radial pattern of macroscopic channels can be generated in core−shell polysaccharide microspheres during gel drying. The mechanical properties and the permeability of the outer crust can be tailored to control the formation of shafts in the organogel. The stiffness of the shell resists the shrinkage of the gel and causes channels to be opened in the direction in which the drying front advances. The permeability of the shell affects the effectiveness of supercritical drying and allows one to control the syneresis of the gel. Examples are provided from a chitosan−silica composite and from Cu-alginate gel beads with chemically modified outer crust.

Introduction

Ionotropic or thermotropic gelations of drops of polysaccharide solution are efficient methods to prepare monodisperse gel microspheres which find widespread application as drug-delivery systems, enzyme carriers for detergency, or supports for biocatalysts.[1−3] The choice of the appropriate polysaccharide allows tailoring of the controlled-release systems adapted to diverse administration conditions. Chitosan, obtained by deacetylation of the chitin from crab shells or squid pens, is a poly-β-D-glucosamine and presents up to 6 mmol g^{-1} of exchangeable amino groups.[4−7] Alginate, extracted from several red seaweeds, is a block copolymer of β-D-mannuronic acid and α-L-guluronic acid.[8−10] It presents carboxylic acid groups and a cation exchange capacity up to 5.6 mmol g^{-1}.

The texture of the polysaccharide gel plays a key role in the kinetics of drug release as well as for more recently proposed applications, such as supports for catalysts in fine chemistry reactions[11] or live tissue reconstruction.[12] A void fraction often higher than 99% affords an exceptional accessibility to the macroporous cavities between the polysaccharide fibrils. The stability of a biocatalyst and the release properties of a drug-carrier system can be optimized by coating the microspheres with polymers leading to a core−shell structure.[13,14] In another preparation method, gelification can be directed to form hollow microcapsules.[15−18] Tthe influence of the polymer nature and the drug−polymer interactions on the release properties have been extensively studied, but little is known about the influence of the drying process and conditions, specially concerning the core−shell microspheres.

Heterogeneities inside the gel microspheres are expected to affect diffusion and swelling phenomena and can explain instances of irreproducible results. A frequent heterogeneity is the formation of a shell with higher gel density at the rim of the microsphere.[19,20] Such a feature considerably improves the retention of cells in biocatalysts. Radial shafts in the depth of the microsphere have been reported as another heterogeneity of alginate gels formed in the presence of copper cations or concentrated calcium cations.[21]

A mechanism for the formation of capillaries normal to the gelation front has been proposed in the case of alginate

* To whom correspondence should be addressed. E-mail: direnzo@enscm.fr.
† Present address: Chimie de la Matière Condensée, UMR 7574, Université Pierre et Marie Curie, Paris, France.

(1) Yao, K.; Peng, T.; Tin Y.; Xu, M.; Goosen, M. F. A. *J. Macromol. Sci.-Rev. Macromol. Chem. Phys.* **1995**, *C35*, 155.
(2) Becker, T.; Park, G.; Gaertner, A. L. In *Enzymes in Detergency*; Van Ee, J. H., Misser, O., Baas, E, Eds.; Marcel Dekker: New York, 1997; p 299.
(3) Kim, S. W.; Bae, Y. H.; Okano, T. *Pharm. Res.* **2002**, *9*, 283.
(4) Domard, A.; Roberts, G. A. F.; Varum, K. M. *Advances in Chitin Science*; Jacques André: Lyon, 1998.
(5) Ravi Kumar, M. N. V.; Muzzarelli, R. A. A.; Muzzarelli, C.; Sashiwa, H.; Domb, A. J. *Chem. Rev.* **2004**, *104*, 6017.
(6) Berger, J.; Reist, M.; Mayer, J. M.; Felt, O.; Peppas, N. A.; Gurny, R. *Eur. J. Pharm. Biopharm.* **2004**, *57*, 19.
(7) Berger, J.; Reist, M.; Mayer, J. M.; Felt, O.; Gurny, R. *Eur. J. Pharm. Biopharm.* **2004**, *57*, 35.
(8) Sandford, P.; Baird, J. In *The polysaccharides*, vol. 2; Academic Press: New York, 1983; p 411.
(9) Sime, W. J. In *Food Gels*; Harris, P., Ed.; Elsevier: Amsterdam, 1990; p 53.
(10) Chen, J. P.; Hong, L.; Wu, S.; Wang, L. *Langmuir* **2002**, *18*, 9413.
(11) Quignard, F.; Choplin, A.; Domard, A. *Langmuir* **2000**, *16*, 9106.
(12) Miralles, G.; Baudoin, R.; Dumas, D.; Baptiste, D.; Hubert, P.; Stoltz, J. F.; Dellacherie, E.; Mainard, D.; Netter, P.; Payan, E. *J. Biomed. Mater. Res.* **2001**, *57*, 268.
(13) Sinha, V. R.; Singla, A. K.; Wadhawan, S.; Kaushik, R.; Kumria, R.; Bansal, K.; Dhawan, S. *Int. J. Pharm.* **2004**, *274*, 1.
(14) Bartkowiak, A.; Hunkeler, D. *Colloid Surf. B* **2001**, *21*, 285.
(15) Blandino, A.; Macias, M.; Cantero, D. *Biosci. Bioeng.* **1999**, *88*, 686.
(16) Bartkoviak, A.; Hunkeler, D. *Chem. Mater.* **2000**, *12*, 206.
(17) Shchukin, D. G.; Suknorukov, G. B.; Möhwald, H. *Angew. Chem., Int. Ed.* **2003**, *42*, 4472.
(18) Cheng, D.; Xia, H.; Chan, H. S. O. *Langmuir* **2004**, *20*, 9909.
(19) Nava Saucedo, J. E.; Audras, B.; Jan, S.; Bazinet, C.E.; Barbotin, J. N. *FEMS Microbiol. Rev.* **1994**, *14*, 93.
(20) Thu, B.; Gåserød, O.; Paus, D.; Mikkelsen, A.; Skjåk-Bræk, G.; Toffanin, R.; Vittur, F.; Rizzo, R. *Biopolymers* **2000**, *53*, 60.
(21) Barbotin, J. N.; Nava Saucedo, J. E. In *Polysaccharides*; Dumitriu, S., Ed.; Marcel Dekker: New York, 1998; p 749.

10.1021/cm0503477 CCC: $30.25
Published on Web 07/29/2005

gelation by divalent cations.[22−24] The mechanism of gelation implies a countercurrent diffusion of the solutions of the polysaccharide and the gelling agent. For appropriate values of the ratio between diffusivity and gelling rate, convection cells are formed, through which the solution of gelling cation can feed the advancing gelation front. In the case of gelation of an alginate solution at the interface with a Cu^{2+} solution, the rising channels of the convection cells may remain in the final gel as a system of parallel void channels normal to the gelation front.[23,24]

The formation of the dense outer shell as well as the radial shafts have been related to the same factors, viz. high concentration of the gelling cations and use of copper instead of calcium cations.[21] This observation was the starting point of our investigation on the influence of a rigid shell on the formation of channel structures in the polysaccharide core. Core−shell microspheres with improved diffusivity inside the macroporous core can present intermediate properties between currently used core−shell systems and hollow shell microcapsules, extending the range of materials available for biocatalysis and drug delivery.

Our strategy to form cavities in the core of polysaccharide beads was not focused on the formation of the polysaccharide gel but on its modification by dehydration treatments. Cavities were generated by controlled syneresis of the core in the presence of a shell able to prevent an isotropic shrinking of the bead. The method has demonstrated a general validity, as several routes for shell formation and several levels of core syneresis have produced systems of radial shafts. Rigid shells have been formed both by chemical modification of the surface of the gel bead or by coating of the bead with a layer of silica gel. Spontaneous contraction of the gel during drying has provided the driving force for shaft openings. Supercritical drying of the gels has allowed characterization of the texture of the beads by the usual techniques of materials science, such as scanning electron microscopy and nitrogen adsorption.

Experimental Section

Preparation of Gel Beads. Chitosan gel beads were formed from an aqueous solution of chitosan (France-Chitine from squid pen, degree of acetylation 10% as measured by IR spectroscopy,[25] Mw 500000 Da) obtained by dissolving 1 g of chitosan in 100 mL of a 0.055 M acetic acid solution. Total dissolution was obtained by stirring overnight at room temperature. Gelation was obtained by dropping the chitosan solution into a 4 M NaOH solution through a 0.8 mm gauge syringe needle. The chitosan beads were left in the alkaline solution for 2 h, filtered, and washed.

To prepare the chitosan−-silica composite, 2 g of chitosan gel beads were introduced into a 25 mL Wheaton flask. A sol formed by water (17 mL), TEOS (0.0566 mmol), and NaF (50 mg) was added to the flask. Mixing was ensured by rotation of the flask around its horizontal axis on a Heidolph Reacx2 stirrer for 12 h. The hybrid beads were then washed with water.

To prepare the copper alginate gel, sodium alginate (Sigma medium viscosity from brown algae, viscosity 3500 cps for a 2 wt % aqueous solution at 20 °C) was dissolved in distilled water at a concentration of 1% (w/w). The polymer solution was added dropwise at room temperature to a stirred $Cu(NO_3)_2$ (Aldrich) solution (0.24 M) using a syringe with a 0.8-mm-diameter needle. The gel beads were left in the gelation solution for a given time. A fraction of the gel beads were filtered and washed with distilled water.

Mineralization of copper alginate was induced by dropwise addition of a 0.48 M NaOH solution to an aqueous solution containing gel beads aged for 3.5 h. Addition of the alkali solution was continued until pH 9 was reached. The beads were left for 2.5 h in the alkaline solution, filtered, and washed. Two types of mineralization treatment were differentiated by the previous washing of the gel beads. For type I treatment, the gel beads were water-washed before mineralization. For type II treatment, the mineralizing solution was directly added to the gelation bath.

Supercritical drying of the gel beads was preceded by dehydration in a series of successive ethanol−water baths of increasing alcohol concentration (10, 30, 50, 70, 90, and 100%) for 15 min each.[26] The gel beads were then dried under supercritical CO_2 conditions (slightly beyond 73 bar and 31.5 °C) in a Polaron 3100 apparatus.

Characterization of Materials. Scanning electron micrographs (SEM) of the dried beads were obtained on an Hitachi S-4500 apparatus after platinum metallization.

Nitrogen adsorption/desorption isotherms were recorded in a Micromeritics ASAP 2010 apparatus at 77 K after outgassing the sample at 323 K under vacuum until a stable 3×10^{-5} Torr pressure was obtained without pumping. Surface area and micropore volume were evaluated by the BET method by assuming a monolayer N_2 molecule to cover 0.162 nm^2. The void fraction was evaluated by subtracting the volume occupied by silica and polymer fibrils from the volume of a gel particle. Densities of 2.2 for amorphous silica[27] and 1.0 for nonexchanged polysaccharide were assumed.

Thermogravimetric analyses were performed with a Netzsch TG 209 C apparatus in air flow at a heating rate 5 °C/min. The amount of organics in the composite was evaluated from the loss of weight at temperature higher than 200 °C. The local composition on gel cross sections was analyzed by an EDX microprobe on a Cambridge Stereoscan 260 apparatus.

Results

Chitosan−Silica Composites. Beads with nearly 3-mm diameter are obtained from drops of chitosan solution by gelling in an alkaline solution. The chitosan hydrogel is very open, with a macroporous void volume of 98%, and can easily be impregnated by a silica sol. Protracted stirring in a silica sol allows a shell of silica gel to be deposited on the outer surface of the beads. Silica-coated chitosan beads are depicted in Figure 1a.

The distribution of silica inside the beads is reported in Figure 2, as measured by EDX microprobe analysis along a cross section. An outer shell 200-μm thick contains only silica. Below this depth, the core of the bead is composed of 80% silica and 20% polysaccharide. These data are in good agreement with the thermogravimetric analysis, which indicates an overall organic content of 16%. The silica shell can be observed by scanning electron microscopy, as in Figure 1b, where it appears as a smooth 200-μm-thick corona at the rim of the bead cross section.

(22) Thumbs, J.; Kohler, H. H. *Chem. Phys.* **1996**, *208*, 9.
(23) Treml, H.; Kohler, H. H. *Chem. Phys.* **2000**, *252*, 199.
(24) Treml, H.; Voelki, S.; Kohler, H. H. *Chem. Phys*. **2003**, *293*, 341.
(25) Hirai, A.; Odani, H.; Nakajima, A. *Polym. Bull.* **1991**, *26*, 17.
(26) Martinsen, A.; Storrø, I.; Skjåk-Bræk. G. *Biotechnol. Bioeng.* **1992**, *39*, 186.
(27) Iler, R. K. *The Chemistry of Silica*; Wiley: New York, 1979.

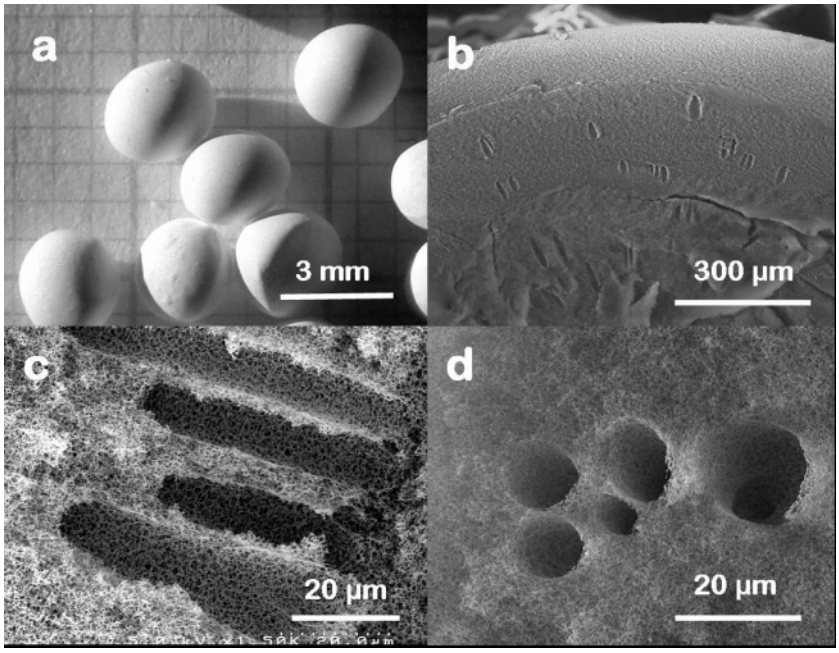

Figure 1. Chitosan−silica composite. (a) Picture of the beads; (b−d) SEM micrographs of cross sections of the beads.

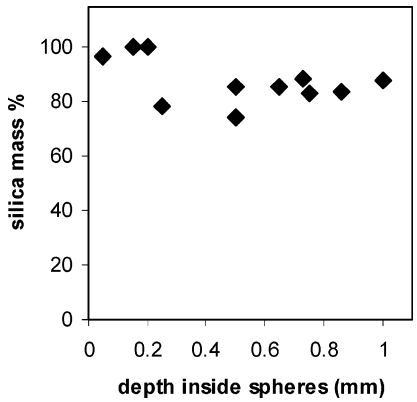

Figure 2. Concentration profile of silica inside chitosan−silica composite beads. Data on a dry basis.

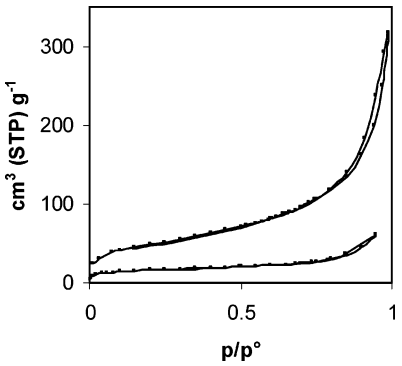

Figure 3. N_2 adsorption isotherms of chitosan aerogel (top) and chitosan−silica composite (bottom).

A radial pattern of channels with an average diameter of 10 μm can be observed in the same micrograph of Figure 1b. No shaft (as the orientation toward the center of the bead allows definition of the channels) can be observed in the silica shell. The shafts do not reach the outer surface of the sphere, but appear to run from the inner surface of the silica shell toward the center of the bead. Details of the shafts can be observed in Figures 1c and 1d. In Figure 1c the shafts are cut by the cross section at a small angle with their axes, while the cross section of Figure 1d is nearly perpendicular to the axes of the shafts. Clusters of shafts are frequently observed. In Figures 1c and 1d the micrometric network of the silica-coated chitosan fibrils can be easily observed, both on the cross section and on the walls of the shafts. This indicates that the macroporosity of the gel and the larger macroporosity represented by the shafts form one pore system.

The N_2 adsorption isotherms of the supercritically dried silica−chitosan composite and corresponding chitosan precursor gel are reported in Figure 3. Both isotherms are essentially type II, corresponding to macroporous solids with high surface area. The BET surface area is 175 $m^2\ g^{-1}$ for the chitosan aerogel and 56 $m^2\ g^{-1}$ for the composite. The much lower surface area of the composite can be attributed to the presence of an 84% silica fraction.

The average size of the composite beads is reported in Table 1, before and after the CO_2 supercritical drying. While the composite beads present no overall shrinking upon drying, a significant size reduction can be observed for beads of chitosan alone. The authors observed no system of radial shafts in chitosan beads without silica or in silica−chitosan composites in which no rigid shell was formed. The formation of the shafts is correlated to the presence of a rigid shell. It seems likely that the shell allows the gel to resist the adhesion forces which normally cause the bead to shrink. The opening of shafts would substitute for bead shrinking and provide an alternative mechanism to decrease the gel volume.

The volume fraction occupied by the shafts can be calculated by pore counting on sections normal to the pore axis. In the case of the composite beads described in this paper, the shafts represent 6% of the gel volume (Table 1).

Cu-Alginate. Beads of Cu-alginate hydrogel and the corresponding aerogel dried after 22 h of aging are represented, respectively, in Figures 4a and 4b. A significant

Table 1. Average Textural Features of the Beads

	shaft diameter (μm)	shaft volume fraction	hydrogel bead size (mm)	aerogel bead size (mm)	bead volume shrinking[a]	gel volume shrinking[a]
chitosan−silica composite	10	0.063	2.80	2.80	0.00	0.06
Cu-alginate aged 22 h	11	0.179	2.80	2.35	0.41	0.52
mineralized Cu-alginate type I	7	0.175	2.40	1.43	0.79	0.82
mineralized Cu-alginate type II	13	0.830	2.44	1.39	0.82	0.97

[a] Volume shrinking $= 1 - (V/V^0)$.

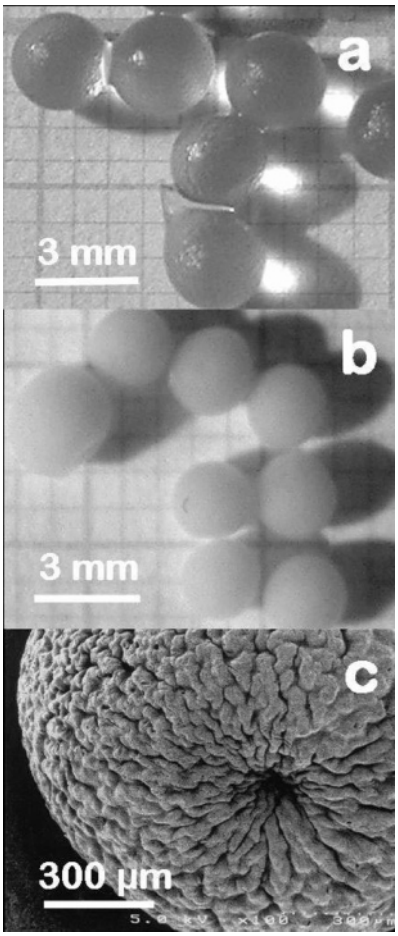

Figure 4. Cu-alginate gel. (a) Picture of the hydrogel beads; (b) picture and (c) SEM micrograph of the aerogel dried after 22 h of aging of the hydrogel.

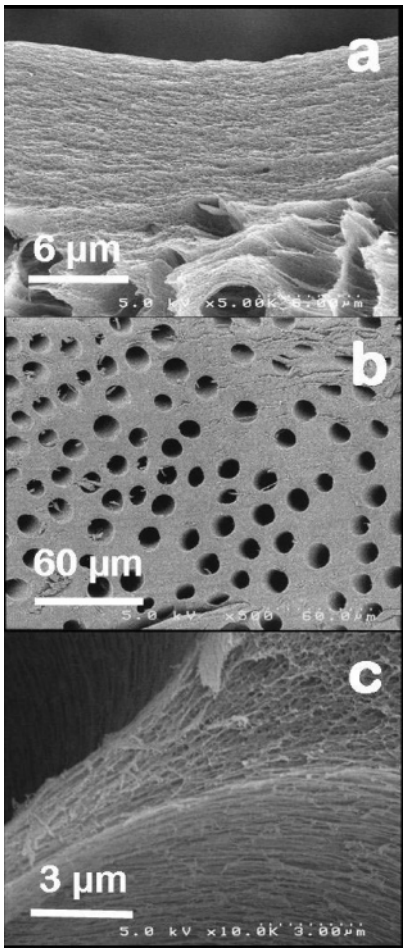

Figure 5. Cu-alginate aerogel dried after 22 h of aging of the hydrogel. SEM micrographs of the cross section of a gel bead.

shrinking of the beads takes place during the dehydration process (Table 1). The average diameter of the gel beads is 2.8 mm for the hydrogel, 2.7 mm for the intermediate alcogel, and 2.35 mm for the supercritically dried aerogel. The overall loss of volume in the hydrogel−aerogel transformation is nearly 40%. The aerogel beads present an extremely rough surface, as depicted in Figure 4c. This shrinked-apple morphology has been reported to be typically formed when alginate is gelified by Cu^{2+} cations.[28]

The presence of a dense outer layer has also been reported to be typical of Cu-alginate gels.[21,28] A section of this crust is shown in Figure 5a. This outer shell is formed by a flattened felt of matted fibrils, densified by the radial retraction of the gel. Below the dense shell, the core presents a thick radial pattern of shafts. In Figure 5b, a cross section normal to the shaft axis is represented. The average diameter of the shafts is 11 μm and they represent nearly 18% of the gel volume. In Figure 5c, a detail of the shaft walls and of a section of the gel near a shaft are presented. The macroporous cells among alginate fibrils are flattened. This indicates that the formation of the shaft has corresponded to an anisotropic contraction of the gel away from the shaft axis. Once the shrinking of the bead and the formation of the shafts are taken into account, the aerogel volume is nearly half the volume of the hydrogel. Notwithstanding this contraction, the void fraction of the aerogel is still higher than 45%.

It is worth noting that no shaft system can be observed in Ca and Co-alginate gels prepared with the same procedure. In the case of Cu-alginate, albeit an outer shell of matted fibrils is already formed at the beginning of the gelation, this does not imply the immediate formation of shafts. The outer shell stiffens during the aging of the gel. No shafts can be observed after 6 h of aging while a complete shaft system is observed after 22 h.

(28) Velings, N. M.; Mestdagh, M. M. *Polym Gels Networks* **1995**, *3*, 311.

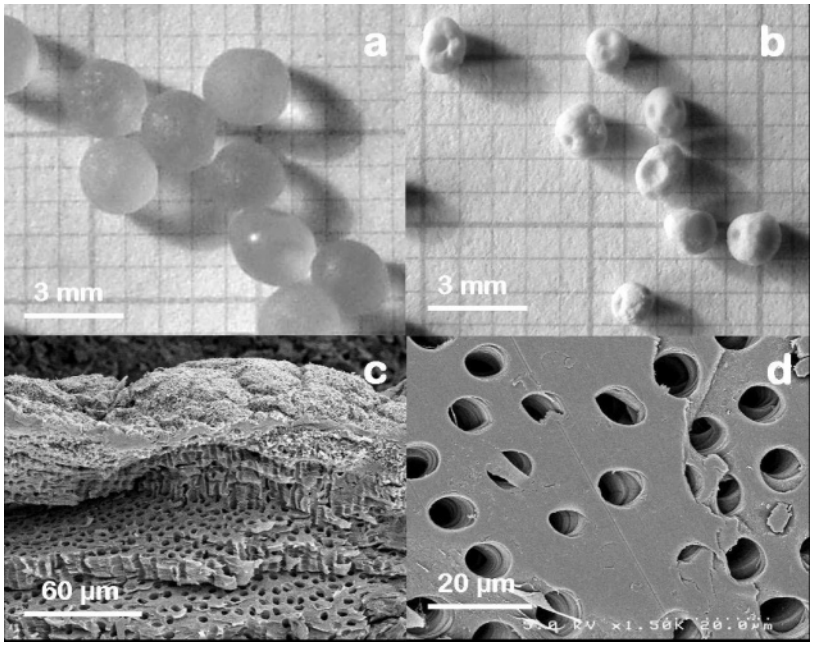

Figure 6. Mineralized Cu-alginate gel (type I). Pictures of (a) hydrogel and (b) aerogel; SEM micrographs of (c) broken aerogel bead and (d) cross section of the aerogel.

Mineralized Cu-Alginate. The crust of the alginate beads can be further stiffened by a mineralization treatment in which the Cu^{2+} cations are displaced by an alkaline solution and precipitate as copper nitrate hydroxide $Cu_2(NO_3)(OH)_3$ at the outer surface of the bead. The crust of basic copper salt is quite water-tight and completely modifies the stability of the beads. While a normal alginate hydrogel shrinks to a nonporous xerogel after overnight exposure in dry air, evaporation from mineralized Cu-alginate is so impaired that the beads retain their water content several days after filtration. For instance, Cu-alginate beads mineralized according to method I are depicted in Figure 6a after 6 days in open air.

The water-tight crust is expected to affect the alcohol exchanges which represent the preliminary steps of the supercritical drying treatment. Indeed, in this case supercritical drying brings about a significant shrinking of the beads, as evidenced by the picture of the aerogel in Figure 6b. The aerogel beads present several pits, where the crust has yielded to the traction of the contracting gel and inverted its curvature. Beads can be easily broken along concentrical coronae, as represented in Figure 6c. A system of radial shafts penetrates the whole volume under the outer crust and represents about 18% of the bead volume. Taking into account both the shrinking of the beads and the loss of gel volume corresponding to the shaft opening, the aerogel retains nearly 20% of the hydrogel volume (Table 1). The surface area of the aerogel is scantily affected by the method I mineralization. Surface areas for the mineralized sample is 496 $m^2\ g^{-1}$, to be compared with the 670 $m^2\ g^{-1}$ surface area of the precursor Cu-alginate aerogel.

Mineralization method II provides a tighter crust of basic copper salt. Beads of Cu-alginate hydrogel and aerogel treated by this method are represented in Figures 7a and 7b, respectively. The shrinking of the gel during the drying treatment induces a polygonal deformation of the beads. The limiting case of deformation is a tennis-ball configuration in which two bilobates surfaces sink toward the center of the bead and leave a protruding ridge between them. The salt crust is quite brittle and easily breaks down. The polysaccharide network no longer occupies the whole bead. The center of the bead is empty and the polysaccharide is concentrated in a fluffy layer under the outer crust.

The polysaccharide layer consists of a radial system of shafts whose diameter increases toward the center of the bead, as shown in Figure 7c. The shafts occupy more than 80% of the polysaccharide layer. In the inner part of the alginate layer, the shafts form a true disordered honeycomb, with coordination of channels between 5 and 7, as shown in Figure 7d. If the shrinking of the beads and the formation of the shafts are taken into account, the dried alginate gel only represents 3% of the volume of the original hydrogel (Table 1). It is clear that mineralization method II has virtually prevented the water−alcohol exchange and the supercritical drying process has been unable to preserve the texture of the polysaccharide gel.

Discussion

The preservation of the texture of organogel beads in the absence of the aqueous solvent is often a critical step for the preparation of porous controlled-release systems. Under evaporative drying, most polysaccharide hydrogels shrink to xerogel with no porosity left. Core−shell beads or capsules usually collapse under evaporative drying into lentil-shaped vesicles. In the case of alginate and chitosan gels, alcohol exchange and CO_2 supercritical drying have proved to be effective methods to preserve the volume and the microscopical texture of the gel.[29,30] However, the presence of a

(29) Valentin, R.; Molvinger, K.; Brunel, D.; Quignard, F. *New J. Chem.* **2003**, *27*, 1690.

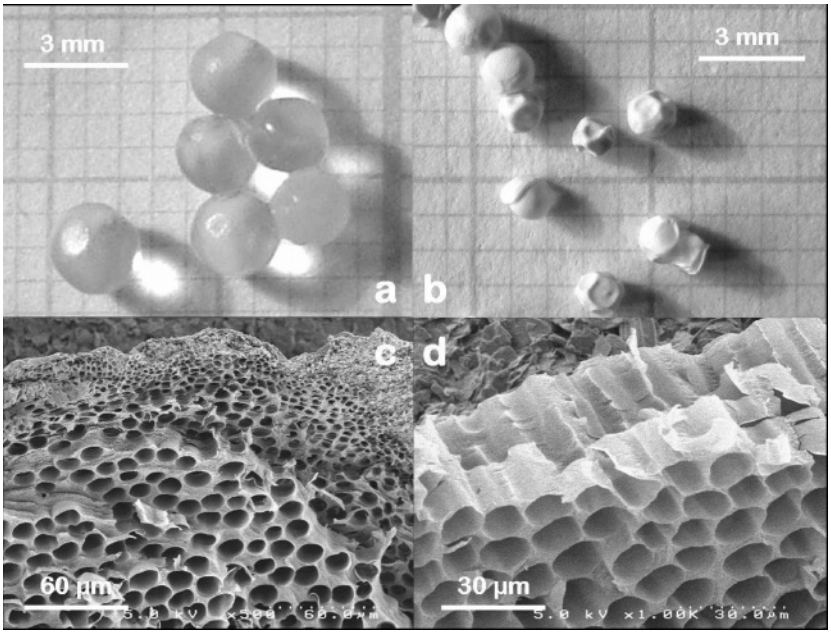

Figure 7. Mineralized Cu-alginate gel (type II). Pictures of (a) hydrogel and (b) aerogel; (c, d) SEM micrographs of broken aerogel beads.

dense shell around the bead can impair the effectiveness of the solvent exchanges which represent the preliminary step of supercritical drying. If some alcohol or, worse, some water is retained in the gel at the moment of the CO_2 extraction, a solvent−vapor interface exerts a traction on the network of the organogel and makes the polysaccharide fibrils adhere to one another.[31] If the outer shell is noncompliant and resists the decrease of the core volume, the gel can be shredded under its own traction and cavities can be opened inside the bead. In this way, both the permeability and the stiffness of the outer shell influence the properties of the dried core.

The gel shrinkage for core−shell beads prepared according to several methods is reported in the last column of Table 1. The macroporous silica shell of the chitosan−silica composite is permeable to liquid and gases and does not affect the effectiveness of the supercritical drying, allowing a very limited gel shrinkage. In the case of Cu-alginate, the outer polysaccharide crust becomes less permeable to fluids with aging and after 22 h of aging it is tight enough to significantly hinder the supercritical drying and lead to about 50% gel shrinking. Mineralization strongly decreases the permeability of the outer crust, and the shrinkage of the gel correspondingly increases.

The influence of a rigid shell on the behavior of the underlying core is quite common in polymer science. For instance, a rigid shell formed of cross-linked pNIPAm (poly-*N*-isopropylacrylamide) has been reported to prevent the volume variation of a core composed of cross-linked pNIPAm-*co*-acrylic acid.[32] Indeed, the formation of cavities is an expected result in the case of a gel syneresis constrained by a noncompliant shell. However, the formation of an ordered radial pattern of channels is quite unexpected and is worth some discussion. The opening of a system of parallel channels has been observed in the gelling of a solution of Na-alginate at the interface with a Cu^{2+} solution.[22,23] The formation of channels depends on the contraction of the gel, which occupies a smaller volume than the parent polysaccharide solution. The channels are perpendicular to the gelation front and correspond to convection cells through which the copper solution can reach the unreacted alginate solution. Formation of channels is observed when the rate of gelling exceeds the diffusion rate of the polysaccharide in a homogeneous system.[24]

In the preparations examined in this paper, no channels are formed during the gelation process. The opening of shafts is only observed during drying of the core−shell systems. The drying process can be expected to begin at the outer surface of the beads and to continue by the advancement of a drying front toward the center of the sphere. The beginning of the drying-related shrinkage at the outer rim of the core is resisted by the adhesion of the gel to the outer crust. The limit tensional stress of the gel is locally reached and the relaxation of the strained gel around the yield point opens a cavity which grows as a shaft when the drying front moves toward the center of the bead. The gel of polysaccharide fibrils becomes anisotropic in the process, as the tridimensional stress of shrinkage originates a bidirectional strain in a plane tangential to the drying front. The contraction of the gel in a direction normal to the shaft axis can be easily observed in Figure 5c.

If the shrinkage continues to a complete densification of the gel, a neat honeycomb pattern is formed, as observed in Figure 7. The formation of hexagonal patterns is commonly associated with drying phenomena at a different scale, like in geological phenomena. Systems of parallel hexagonal columns are often formed by the drying of clay beds or the cooling of basalt flows. In these cases, the contraction of the material brings about a periodical nucleation of cracks and the formation of a regular pattern. The polysaccharide

(30) Valentin, R.; Molvinger, K.; Quignard, F.; Di Renzo, F. *Macromol. Symp.* **2005**, *222*, 93−101.
(31) Brinker, C. J.; Scherer, G. W. *Sol−Gel Science*; Academic Press: Boston, 1990; p 458.
(32) Jones, C. D.; Lyon, L. A. *Langmuir* **2003**, *19*, 4544.

honeycombs observed in mineralized Cu-alginate can be correspondingly described as void columns separated by films formed by the adhesion of the organic fibrils.

Cu-alginate and chitosan−silica composites seem to be only instances of a more general behavior of core−shell systems. Indeed, the formation of a radial pattern of shafts seems to be independent of the nature of the organogel or the composition of the crust and similar results can be expected from any core−shell system with similar mechanical and permeation properties. The opening of the macroscopic shafts inside an already macroporous gel gives rise to a system with a hierarchical porosity and a very high accessibility. Paradoxically, the improved permeability of the core is related to a significant decrease of permeability of the outer shell. However, the presence of a tight shell is a bonus for controlled-release applications and the porosity of the core can contribute to a rapid release once the outer shell decomposes in the area of therapeutical targeting. This can solve frequently encountered problems related to the heterogeneous distribution of drugs inside the beads.[33] It seems relatiely easy to extend the method to the shaping of different biopolymer objects, like the rafts or tablets used in several drug-delivery systems.[34] In the case of catalytic applications, a permeable core in core−shell system can bring about a rapid homogeneization once a reagent has passed the potential barrier of the outer shell.

In a general way, the transport properties of core−shell systems with radial shafts can be compared to the properties of microcapsules, with the additional advantage of a large internal surface for the stabilization of active groups.

Acknowledgment. The authors gratefully acknowledge the help of D. Cot and N. Masquelez for electron microscopy.

CM0503477

(33) Berkland, C.; Kim, K. K.; Pack, D. W. *Pharm. Res.* **2003**, *20*, 1055.
(34) Tønnesen, H. H.; Karlsen, J. *Drug Dev. Ind. Pharm.* **2002**, *28*, 621.